A new glucagon and GLP-1 co-agonist eliminates obesity in rodents

Jonathan W Day[1], Nickki Ottaway[2], James T Patterson[1], Vasily Gelfanov[1], David Smiley[1], Jas Gidda[3], Hannes Findeisen[4], Dennis Bruemmer[4], Daniel J Drucker[5], Nilika Chaudhary[2], Jenna Holland[2], Jazzminn Hembree[2], William Abplanalp[2], Erin Grant[2], Jennifer Ruehl[2], Hilary Wilson[2], Henriette Kirchner[2], Sarah Haas Lockie[2], Susanna Hofmann[6], Stephen C Woods[2], Ruben Nogueiras[2], Paul T Pfluger[2], Diego Perez-Tilve[2], Richard DiMarchi[1] & Matthias H Tschöp[2,6]

We report the efficacy of a new peptide with agonism at the glucagon and GLP-1 receptors that has potent, sustained satiation-inducing and lipolytic effects. Selective chemical modification to glucagon resulted in a loss of specificity, with minimal change to inherent activity. The structural basis for the co-agonism appears to be a combination of local positional interactions and a change in secondary structure. Two co-agonist peptides differing from each other only in their level of glucagon receptor agonism were studied in rodent obesity models. Administration of PEGylated peptides once per week normalized adiposity and glucose tolerance in diet-induced obese mice. Reduction of body weight was achieved by a loss of body fat resulting from decreased food intake and increased energy expenditure. These preclinical studies indicate that when full GLP-1 agonism is augmented with an appropriate degree of glucagon receptor activation, body fat reduction can be substantially enhanced without any overt adverse effects.

Obesity and its associated consequences, including adult-onset diabetes, remain a primary health and economic threat for modern societies[1]. Pharmacologic treatment that is efficacious and safe has yet to emerge, but the enhanced acceptance of obesity as a chronic disease has elevated the search for a suitable new therapy[2]. Surgical interventions such as gastric bypass remain the only therapeutic options with curative potential. Currently the most effective drug for treatment of the metabolic syndrome activates the receptor (GLP-1R) for the gut peptide glucagon-like peptide-1 (GLP-1). GLP-1R agonism safely improves glycemic control in people with adult-onset diabetes, with simultaneous reduction in body weight[3,4]. Enhancing pharmacotherapy by combining multiple peptides targeting different receptors is emerging as a viable and attractive approach to treat obesity[5]. Identifying the most effective agents and minimizing the total number of drugs to be used simultaneously constitutes a major research challenge.

Acute glucagon administration reduces food intake in animals[6] and in humans[7], and some reports indicate that sustained glucagon receptor (GCGR) activation not only decreases food intake[8,9] but also promotes lipolysis[10–12] and weight loss[13,14]. Chronic investigation of glucagon's metabolic effects are challenging since the native hormone is rapidly degraded and has poor solubility and stability in physiological buffers. Glucagon and GLP-1 have distinct receptors that are also structurally related[15]. Despite this similarity, glucagon and GLP-1 have classically been thought to oppose each other in controlling blood glucose. Glucagon acts directly at the liver to raise blood glucose by stimulating gluconeogenesis and glycogenolysis, whereas GLP-1 acts by multiple mechanisms to lower glucose, most notably by enhancing glucose-stimulated insulin synthesis and secretion at the pancreas[16]. Another proglucagon gene product, oxyntomodulin, also reduces food intake and body weight in rodents and humans, much like that reported for GLP-1 (refs. 17–20).

Herein we explore the efficacy of combined glucagon and GLP-1 agonism in a single peptide. We hypothesized that the antihyperglycemic property of GLP-1 agonism would minimize any diabetogenic risk of excessive glucagon agonism. The lipolytic and thermogenic properties attributed to glucagon[10,21], in addition to the satiation-inducing pharmacology of GLP-1, provided a strong mechanistic rationale for the development of a synergistic co-agonist peptide. A set of potent glucagon and GLP-1 co-agonists having differing activity at each receptor of interest was synthesized and biochemically characterized *in vitro*. Two specific glucagon analogs enhanced for sustained action and engineered to have activity at the GLP-1R comparable to that of native GLP-1 were studied pharmacologically in rodent obesity models. Weekly administration of PEGylated peptides normalized adiposity and glucose tolerance in diet-induced obese mice. Body weight reduction was achieved by a loss of body fat resulting from decreased food intake and increased energy expenditure. The amount of body weight and fat loss increased with greater glucagon receptor agonism. These co-agonist compounds also normalized glucose and lipid metabolism and reduced liver steatosis.

[1]Department of Chemistry, Indiana University, Bloomington, Indiana, USA. [2]Obesity Research Centre, Department of Psychiatry, University of Cincinnati, Cincinnati, Ohio, USA. [3]Marcadia Biotech, Carmel, Indiana, USA. [4]Division of Endocrinology and Molecular Medicine, University of Kentucky College of Medicine, Lexington, Kentucky, USA. [5]Department of Medicine, Samuel Lunenfeld Research Institute, Mount Sinai Hospital, University of Toronto, Toronto, Ontario, Canada. [6]Division of Endocrinology, University of Cincinnati, Cincinnati, Ohio, USA. Correspondence should be addressed to R.D. (rdimarch@indiana.edu).
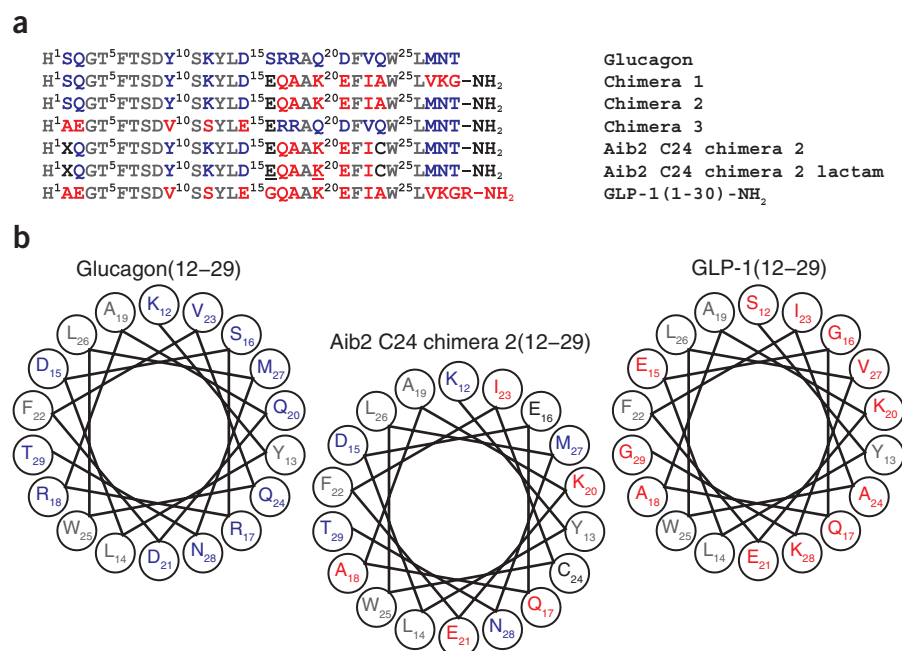
a

```
H¹SQGT⁵FTSDY¹⁰SKYLD¹⁵SRRAQ²⁰DFVQW²⁵LMNT          Glucagon
H¹SQGT⁵FTSDY¹⁰SKYLD¹⁵EQAAK²⁰EFIAW²⁵LVKG-NH₂      Chimera 1
H¹SQGT⁵FTSDY¹⁰SKYLD¹⁵EQAAK²⁰EFIAW²⁵LMNT-NH₂      Chimera 2
H¹AEGT⁵FTSDV¹⁰SSYLE¹⁵ERRAQ²⁰DFVQW²⁵LMNT-NH₂      Chimera 3
H¹XQGT⁵FTSDY¹⁰SKYLD¹⁵EQAAK²⁰EFICW²⁵LMNT-NH₂      Aib2 C24 chimera 2
H¹XQGT⁵FTSDY¹⁰SKYLD¹⁵EQAAK²⁰EFICW²⁵LMNT-NH₂      Aib2 C24 chimera 2 lactam
H¹AEGT⁵FTSDV¹⁰SSYLE¹⁵GQAAK²⁰EFIAW²⁵LVKGR-NH₂     GLP-1(1-30)-NH₂
```

b

Figure 1 Structure of glucagon, GLP-1 and chimeric peptides. (**a**) Amino acid sequence and structure of glucagon and GLP-1 chimerae. Underlined residues indicate site of lactam formation. (**b**) Helical wheel representation of glucagon, GLP-1 and chimeric peptide showing residues 12–29.

RESULTS

Structure-function of glucagon-based co-agonists

Glucagon is a C-terminal peptide acid of 29 amino acids, and bioactive GLP-1 contains 30 or 31 residues terminating in a C-terminal amide or acid, respectively. The N-terminal sequence of these hormones is highly conserved, and positions 2, 3, 10 and 12 are key in maintaining glucagon activity[15,22] (**Fig. 1a**). Notably, the GLP-1R does not distinguish between the two different N-terminal sequences of these two hormones[23]. In contrast, the peptide sequences diverge at 10 of 14 residues in the C-terminal region—amino acids 16–29.

Native glucagon achieves a degree of selectivity from its C-terminal residues, and a significant contribution is made by the C-terminal acid. Substitution with a C-terminal amide provides a backbone with reduced specificity for GCGR. The additional importance of position 16 for stability of the C-terminal helix has been shown through GLP-1 and Ex-4 structural comparison[24]. Incorporation of a series of amino acid substitutions at position 16 of glucagon enabled increased potency at GLP-1R and provided a basis for additional structure-function studies with the goal of achieving balanced co-agonism (**Table 1**).

A division of the native glucagon peptide into two halves pivoting with a common glutamic acid at position 16 was used in the design of a chimeric sequence of high GLP-1 potency (**Fig. 1a**). GLP-1 residues were used in the glucagon sequence at positions 17, 18, 20, 21, 23 and 24 to create a glucagon and GLP-1 chimeric peptide identified as chimera 2. Aminoisobutyric acid (Aib) was inserted at position 2 to provide resistance to cleavage by dipeptidylpeptidase-4 (DPP-4). We introduced a single side chain lactam bridge in the middle of the peptide to stabilize the secondary structure and enhance glucagon agonism. The helical wheel diagram (**Fig. 1b**) reveals the proximity of Glu16 and Lys20 on the hydrophilic face of the helix. These two side chains were covalently coupled in the course of peptide assembly as a side chain amide. This macrocyclization of the peptide represents a 21-atom lactam and is identified

as Aib2 C24 chimera 2 lactam (**Fig. 1**). Finally, site-specific 40-kDa PEGylation was achieved at cysteine residue 24 through reaction with a maleimide-functionalized linear PEG to yield the peptides identified as Aib2 C24 40k and Aib2 C24 lactam 40k. These PEGylated peptides were soluble in physiological buffers at concentrations above 25 mg ml^{-1}, and both PEGylated peptides proved completely resistant to degradation after *ex vivo* incubation with plasma for periods of one week.

Structural assessment of chimeric peptides

We analyzed the structural conformation within this peptide series by circular dichroism (**Fig. 2a**, **Supplementary Fig. 1** and **Supplementary Table 1**), and glucagon proved to be the least helical peptide examined. GLP-1 exhibited a 50% relative enhancement in helicity, demonstrating that these two peptides differ in primary as well as secondary structure. Several glucagon-related peptides of varying bioactivity demonstrated comparable helicity in trifluoroethanol (TFE) concentrations of 30 and 40% (v/v), with the exception of the single lactam analog (**Supplementary Table 1**). At a lower concentration of TFE, the peptide CD spectra differentiated to a greater degree, and the lactam analog was clearly the most helical in structure. The more conservatively substituted analogs of glucagon amide (**Supplementary Table 1**) were virtually indistinguishable from GLP-1 at all TFE concentrations, although they were clearly distinguishable from glucagon (**Fig. 2a**, peptides **1** and **13**; see also **Supplementary Results**). Peptide **5** is the C-terminal acid version of **4** as well as the Glu16 version of peptide **1**. In the absence of TFE and at 10% concentration, the structure appears more related to native glucagon than to the amide-based analogs. Notably, the more liberally substituted analogs, chimera 1 (**14**) and chimera 2 (**15**), had helical structures characteristic of GLP-1 throughout the TFE titration, but not in its absence (**Supplementary Table 1**).

Surprisingly, there were no significant changes in the helicity of the peptides when PEGylated. In contrast, the apparent helicity of the lactam-based peptide (**32**) in phosphate buffer in the absence of TFE was approximately double that of the peptide in its open form (**30**) (36% versus 17%, respectively). Consequently, the PEGylated forms of these two chimeric peptides (**31** and **33**) differed appreciably in secondary structure (**Fig. 2a** and **Supplementary Table 1**), and the differences in biological properties are likely a function of these secondary structural differences.

Receptor-mediated cAMP synthesis

A series of peptide analogs were synthesized ('series 1') with modifications at position 16 of glucagon amide (**Table 1** and **Supplementary Fig. 2**). Each peptide was tested for its ability to stimulate cAMP synthesis via GCGR and GLP-1R in a cell-based reporter gene assay. Native glucagon (**1**) activated GCGR half maximally at an effective concentration (EC$_{50}$) of 0.071 ± 0.036 nM and activated GLP-1R with an EC$_{50}$ of 3.3 ± 0.5 nM. GLP-1$_{1-30}$-NH$_2$ (**2**) activated GLP-1R at an EC$_{50}$ of 0.033 ± 0.017 nM and activated GCGR with an EC$_{50}$ exceeding 1 μM. Addition of the C-terminal amide to glucagon yielded peptide **3** (T29-NH$_2$), which half-maximally stimulated GCGR and GLP-1R at 0.15 ± 0.10 nM and 0.60 ± 0.37 nM, respectively.

Table 1 Glucagon and GLP-1 receptor-mediated cAMP synthesis by glucagon-based analogs

		Peptide	GCGR EC$_{50}$ (nM)	s.d.	GLP-1R EC$_{50}$ (nM)	s.d.	GCGR Relative %	GLP-1R Relative %	Selectivity ratio GCGR:GLP-1R
Series 1	1	Glucagon	0.071	0.036	3.3	0.5	100	1.0	100
	2	GLP-1$_{1-30}$-NH$_2$	>1,000	–	0.033	0.017	<0.1	100	<0.1
	3	T29-NH$_2$	0.15	0.10	0.60	0.37	46	5.5	8.4
	4	E16 T29-NH$_2$	0.049	0.019	0.17	0.11	146	19	7.7
	5	E16 T29-OH	0.053	0.023	1.1	0.5	134	2.9	46
	6	H16 T29-NH$_2$	0.10	0.03	0.23	0.06	70	15	4.8
	7	Q16 T29-NH$_2$	0.071	0.033	0.26	0.17	100	13	7.8
	8	hE16 T29-NH$_2$	0.054	0.014	0.13	0.04	131	25	5.3
	9	hCysSO$_3$16 T29-NH$_2$	0.10	0.03	0.12	0.03	69	28	2.5
	10	D16 T29-NH$_2$	0.068	0.016	0.57	0.14	104	5.8	18
	11	G16 T29-NH$_2$	0.13	0.07	0.58	0.12	54	5.7	9.5
	12	T16 T29-NH$_2$	0.13	0.04	0.58	0.16	57	5.7	9.9
Series 2	13	E16 K20 T29-NH$_2$	0.077	0.026	0.071	0.034	93	47	2.0
	14	Chimera 1	0.47	0.19	0.015	0.009	15	219	<0.1
	15	Chimera 2	0.068	0.029	0.026	0.012	104	128	0.81
	16	E16 Q17 K20 T29-NH$_2$	0.048	0.001	0.075	0.056	149	44	3.4
	17	E16 A18 K20 T29-NH$_2$	0.087	0.018	0.028	0.019	81	117	0.70
	18	E16 K20 E21 T29-NH$_2$	0.068	0.018	0.075	0.030	104	44	2.3
	19	E16 K20 I23 T29-NH$_2$	0.073	0.004	0.068	0.033	97	49	2.0
	20	E16 K20 A24 T29-NH$_2$	0.080	0.001	0.087	0.048	89	38	2.3
	21	Chimera 3	50	17	0.18	0.10	0.10	18	<0.1
	22	E3 E16 T29-NH$_2$	3.7	1.6	0.11	0.05	1.9	31	<0.1
	23	E3 chimera 2	2.4	1.0	0.028	0.011	3.0	120	<0.1
	24	E16 GLP-1-NH$_2$ Des-R30	>1,000	–	0.011	0.003	<0.1	294	<0.1
	25	K20 T29-NH$_2$	0.12	0.04	0.13	0.05	59	25	2.3
Series 3	26	K12 E16 lactam	0.046	0.016	0.051	0.002	155	64	2.4
	27	E16 K20 lactam	0.058	0.032	0.049	0.008	123	68	1.8
	28	K20 E24 lactam	0.078	0.039	0.24	0.10	91	14	6.6
	29	E24 K28 lactam	0.076	0.069	0.18	0.01	94	18	5.1
Series 4	30	Aib2 C24 chimera 2*	0.59	0.12	0.014	0.002	9.4	202	0.046
	31	Aib2 C24 40k*	2.9	1.0	0.036	0.014	1.9	78	0.024
	32	Aib2 C24 chimera 2 lactam*	0.055	0.011	0.013	0.005	100	220	0.45
	33	Aib2 C24 lactam 40k*	0.67	0.26	0.059	0.029	8.2	48	0.17

EC$_{50}$ values represent peptide concentrations at which half-maximum activation is occurring at the glucagon and GLP-1 receptors. A minimum of three separate experiments were conducted for each peptide at the glucagon and GLP-1 receptors. * indicates relative percent values based on glucagon EC$_{50}$ at GCGR of 0.055 nM and GLP-1 EC$_{50}$ at GLP-1R of 0.028 nM. Glucagon receptor, GCGR; GLP-1 receptor, GLP-1R. Relative % at GCGR = (glucagon EC$_{50}$/peptide analog EC$_{50}$) × 100. Relative % at GLP-1R = (GLP-1 EC$_{50}$/peptide analog EC$_{50}$) × 100. Selectivity ratio = (relative % at GCGR)/(relative % at GLP-1R).

Modification of peptide **3** at position 16 resulted in analogs (**4** and **6–12**) with potencies in a range of 54–146% relative to glucagon at GCGR and 5–28% relative to GLP-1 at GLP-1R. This demonstrates the slightly greater sensitivity of GLP-1R relative to GCGR for the changes made at position 16 in the glucagon sequence. Notably, all modifications at position 16 were at least as potent as the native serine at GCGR and GLP-1R. Within this set of analogs, the peptides of greatest potency at GCGR had a carboxylic acid side chain (**4**, **8** and **10**) at position 16. Peptide **4** exhibited 146% potency relative to glucagon at GCGR and 19% relative to GLP-1 at GLP-1R.

To further enhance co-agonism at GCGR and GLP-1R, we synthesized a series of hybrid glucagon-like peptides ('series 2') that use peptide **4** as a reference point. We studied four peptides (**14**, **15**, **21** and **24**) that systematically introduced varying degrees of GLP-1 sequence (**Table 1** and **Supplementary Fig. 3**). The N-terminal 1–15 amino

acid sequence of GLP-1 within peptide **21** (chimera 3) was observed to greatly diminish activity at GCGR and did not improve potency at GLP-1R relative to **4**. Conversely, the presence of C-terminal amino acids 17–29 of GLP-1 in peptide **14** (chimera 1) substantially increased GLP-1 activity beyond that of the native ligand, but considerably reduced potency at GCGR to only 15% of that of native glucagon. Amino acids 27–29 of glucagon, when collectively substituted in peptide **14** to yield peptide **15** (chimera 2), activated GCGR half maximally at a concentration of 0.068 nM and activated GLP-1R half maximally at a concentration of 0.026 nM. This activity profile represents greater potency than the native ligands at both receptors. Consequently, the six amino acid differences between peptide **4** and **15** serve to modestly lower potency at GCGR and substantially increase GLP-1R potency to yield a fully potent co-agonist. Peptide **15** demonstrates that GLP-1R agonism can be inserted at a level comparable
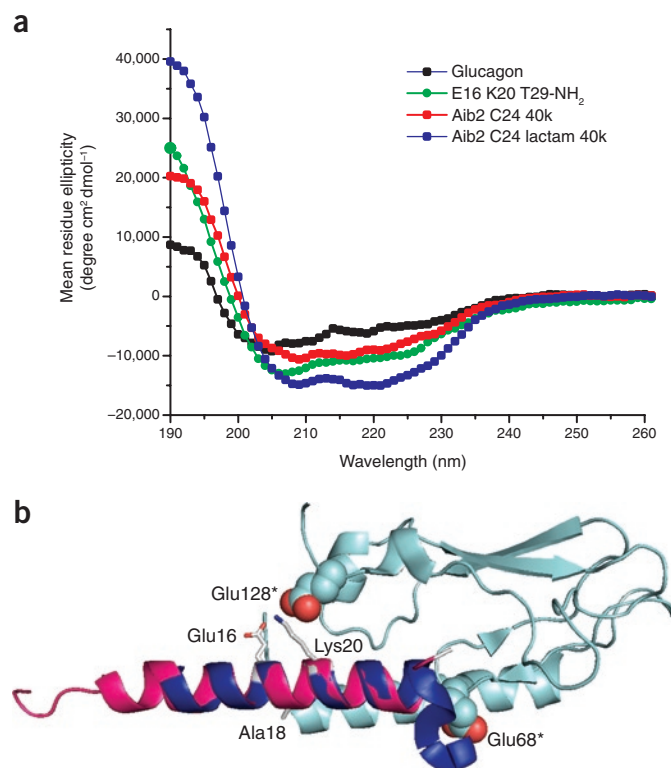
Figure 2 Structure of glucagon-based peptides using circular dichroism and a ligand-receptor model. (**a**) Structural changes of agonists and co-agonists as measured by circular dichroism in 10% TFE. (**b**) Crystal structure of Ex-4(9–39) colored blue with the N-terminal extracellular domain of the GLP-1 receptor in light blue (Protein Data Bank code 3C5T). The crystal structure of glucagon (Protein Data Bank code 1GCN) colored in pink was aligned with Ex-4 in the receptor binding pocket using PyMol (DeLano Scientific LLC). Positions 16, 18, 20 and the C terminus of glucagon are highlighted in white to indicate mutations to those positions achieved in PyMol. Glu128* and Glu68* of the receptor are shown in a space-fill representation (* indicates receptor amino acid).

to that of the native hormone and 100-fold greater than that of native glucagon, without compromising activity at GCGR.

The relative contribution of the GLP-1–derived amino acids at residues 17–24 to the profile of peptide **15** was studied. Addition of Lys20 to peptide **4** yields peptide **13**, a potent GLP-1R agonist with a potency at GCGR that is near that of native glucagon. Peptide **13** has a potency at GCGR that is similar to that of peptide **15** (chimera 2), but peptide **13** is threefold less potent at GLP-1R. Divergent amino acids between

peptides **13** and **15** were modified to yield peptides **16–20** (**Table 1** and **Supplementary Fig. 4**). Each analog retained glucagon potency in the range of 81% to 149% relative to glucagon, whereas GLP-1 receptor activity varied from 38% to 117% relative to GLP-1. The four modifications represented in peptide **17** (Glu16, Ala18, Lys20 and C-terminal amide) are highlighted in a glucagon overlay to the Ex-4 (9–39) GLP-1R N-terminal extracellular domain structure[25] (**Fig. 2b**).

To explore the prospect that the Glu16, Lys20 substitution in multiple high-potency GLP-1R agonists (**13–20** and **23**) was collectively functioning as an ion pair, we studied four additional peptides with a single side chain lactam bridge ('series 3'; **Table 1** and **Supplementary Fig. 5**). Our analysis was performed by inserting a lactam bridge in an *i* to *i* + 4 location in the sequence range of amino acids 12–28. The specific substitutions were Lys12-Glu16 (**26**), Glu16-Lys20 (**27**), Lys20-Glu24 (**28**) and Glu24-Lys28 (**29**). In all instances the lactam analogs displayed increased potency at both receptors relative to peptide **3**, demonstrating that a more stable backbone helix was favorable, independent of the specific attachment point. The relative potency differed in a range of 91–155% at GCGR and 14–68% at GLP-1R. However, the results demonstrate important differences, where central placement of the lactam provided maximal activation at both receptors, with C-terminal placement being somewhat less favorable to GLP-1R. The most substantial increase in potency at GLP-1R to yield nearly balanced co-agonists occurred when the backbone constraint involved amino acid 16 (**26** and **27**). The 12–16 and 16–20 lactam-based glucagon amides were highly potent at GLP-1R while maintaining native glucagon's potency at GCGR.

The GLP-1R responds favorably to the presence of Lys20 (**4** versus **13** and **3** versus **25**) and is further enhanced by lactamization in either location (**13** versus **26** and **27**). The glucagon receptor is not favorably influenced by any of the three changes relative to the single glutamic acid substitution at position 16 (**4**). The lactam peptides **26** and **27** are of comparable activity, and the Lys20 analog is slightly less favored (**13**). It appears that both primary and secondary structure are used to differentiate recognition at these two homologous receptors, with GLP-1R being more sensitive to higher order structural changes in the context of glucagon sequence.

We assessed two DPP-4 protected peptides and their 40-kDa PEGylated derivatives ('series 4') for their potency in cell-based reporter assays (**Table 1** and **Supplementary Fig. 6**). The potency of Aib2 C24 chimera 2 (**30**) at GLP-1R was twice that of native GLP-1 and had activity at GCGR that was approximately 10% that of native glucagon. The introduction of the lactam (**32**) restored full
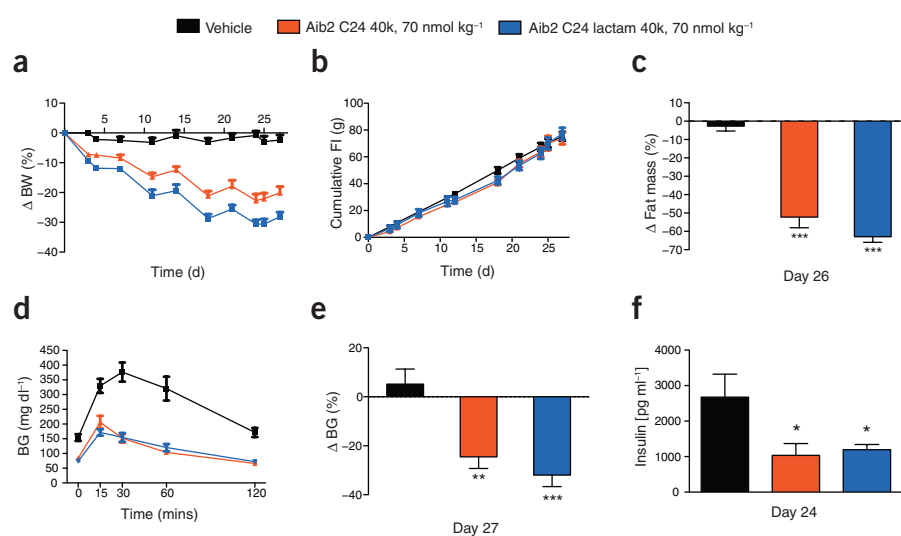

Figure 3 One-month treatment of diet-induced obese mice with glucagon and GLP-1 chimerae Aib2 C24 40k and Aib2 C24 lactam 40k. (**a**–**f**) Effects on body weight (**a**), overall food intake (**b**), body fat mass (**c**), glucose tolerance (**d**), fasting blood glucose (**e**) and total plasma insulin levels (**f**). *$P < 0.05$, **$P < 0.01$, ***$P < 0.001$.
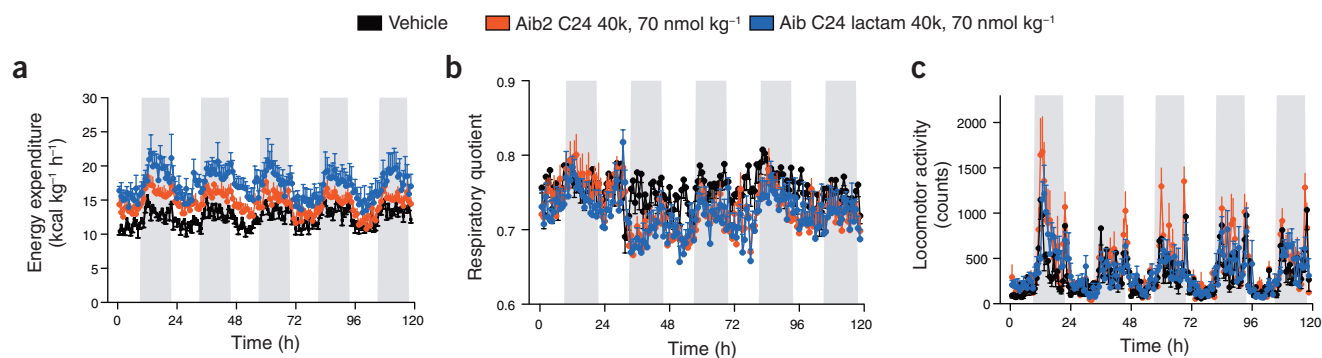
Figure 4 One-month treatment of diet-induced obese mice with glucagon and GLP-1 chimerae Aib2 C24 40k and Aib2 C24 lactam 40k. (**a**) Energy expenditure. (**b**) Respiratory quotient. (**c**) Locomotor activity.

glucagon agonism without a change at GLP-1R. Consequently, Aib2 C24 chimera 2 lactam is a fully potent, nearly balanced co-agonist relative to the native ligands at the two respective receptors. PEGylation of each peptide (**31** and **33**) reduced potency by as much as tenfold at GCGR and fivefold at GLP-1R. The PEGylated peptides were slightly less potent at GLP-1R than native GLP-1 but still had a subnanomolar EC_{50}. The Aib2 C24 40k is sevenfold more selective than the more balanced lactam version of this peptide at the GLP-1R. Therefore, these two DPP-4–resistant peptides are suitable for sustained *in vivo* time-action experiments and well-matched for GLP-1R agonism, but they differ in glucagon agonism.

One-week study in diet-induced obese mice
The 40-kDa PEGylated peptides were administered as single weekly subcutaneous injections in diet-induced obese (DIO) C57B6 mice (**Supplementary Fig. 7**). A single injection of 325 nmol kg^{-1} of the more balanced lactam-based co-agonist decreased body weight over one week by 25.8%, from 50.9 ± 1.4g to 37.8 ± 0.8 g ($P < 0.0001$, $n = 8$ per group) (**Supplementary Fig. 7**). Comparable administration of the unbalanced open-form PEGylated peptide was effective but considerably less potent, as the decrease in body weight was 9% (49.1 ± 1.51 g to 44.68 ± 1.38 g). Saline-injected control mice did not change their body weight (50.61 ± 1.32 g before, 50.87 ± 1.46 g after) (**Supplementary Fig. 7a**). The body weight changes were a result of a decrease in fat mass (41.9% for the balanced lactam peptide, 22.2% for unbalanced open form, 2.3% for controls, $P < 0.001$) (**Supplementary Fig. 7b**) and were paralleled by a significant decrease in average daily food intake (balanced lactam, 0.40 ± 0.29 g d^{-1}; unbalanced open, 1.83 ± 0.81 g d^{-1}; saline, 2.70 ± 0.78 g d^{-1}; $P < 0.0001$) (**Supplementary Fig. 7c**). Blood glucose was significantly decreased for both peptides when compared to control, and slightly more so in the balanced lactam-based peptide (balanced, –90.1 mg dl^{-1}; unbalanced, –79.6 mg dl^{-1}; control, –23.9 mg dl^{-1}; $P = 0.0433$) (**Supplementary Fig. 7d**).

Single subcutaneous injections of six different doses (0, 7, 14, 35, 70, 140 and 350 nmol kg^{-1}) of the unbalanced open-form (**Supplementary Figs. 8a,b**) and balanced lactam-based (**Supplementary Fig. 8c,d**) PEGylated peptides demonstrated linearly responsive, dose-dependent decreases of body weight and blood glucose. The magnitude of the effect was more prominent with the balanced co-agonist peptide, which indicates that the additional element of glucagon agonism improves the potency of the peptide. Importantly, at an efficient dose of 70 nmol kg^{-1}, neither of these two compounds caused acute hypo- or hyperglycemia, in spite of potent agonism at both the GLP-1 and the glucagon receptors (**Supplementary Fig. 8e**).

One-month therapy in DIO mice
In a follow-up experiment, we tested the effect of weekly subcutaneous injections of 70 nmol kg^{-1} of Aib2 C24 lactam 40k or Aib2 C24 40k (**Fig. 3**). The injections decreased body weight of DIO mice by 28.1% and 20.1%, respectively ($P < 0.0001$, $n = 7$ or 8 per group) (**Fig. 3a**). The body weight changes were associated with a decrease in fat mass (–62.9% for Aib2 C24 lactam 40k, –52.2% for Aib2 C24 40k, and 5.1% for controls, $P < 0.0001$) (**Fig. 3c**). Notably, long-term effects of these lower doses on food intake ($P = 0.95$) (**Fig. 3b**) were not statistically significant. Energy expenditure, however, was increased with Aib2 C24 lactam 40k (17.19 ± 1.49 kcal/(kg h)) and Aib2 C24 40k (14.60 ± 0.69 kcal/(kg h)) compared to vehicle (12.71 ± 0.45 kcal/(kg h); $P = 0.0187$), and the respiratory quotient tended to be decreased (**Fig. 4a,b**) (0.719 ± 0.01 for Aib2 C24 lactam 40k, 0.725 ± 0.01 for Aib2 C24 40k, and 0.755 ± 0.01 for vehicle; $P = 0.1028$), which indicates that increased thermogenesis and altered nutrient partitioning may explain the overall negative energy balance. Increased energy expenditure was not associated with a change in spontaneous physical activity–induced thermogenesis (NEAT) since locomotor activity did not differ between treatment groups and controls ($P = 0.4281$) (**Fig. 4c**). Neither automated online monitoring of acute feeding nor chronic monitoring of food intake revealed any differences in caloric intake (automated $P = 0.667$, chronic $P = 0.9484$) (**Supplementary Fig. 9a–e**).

Blood glucose levels were markedly decreased over the treatment period starting at day 3 after the first injection (mean decrease: Aib2 C24 lactam 40k, –32%; Aib2 C24 40k, –24.5%; controls, –2.7%; $P < 0.0001$) (**Fig. 3e**). In response to an intraperitoneal glucose challenge on day 3, blood glucose peaks (**Fig. 3d**) and profiles (AUC) (**Supplementary Fig. 9f**) were markedly lower in the two treated groups (Aib2 C24 lactam 40k, 14,183 ± 1,072; Aib2 C24 40k, 13,794 ± 824.1) compared to the vehicle-treated controls (34,125 ± 3,142, $P < 0.0001$). After one month of treatment with Aib2 C24 lactam 40k or Aib2 C24 40k, plasma insulin was lower in the treatment groups (1,194 pg ml^{-1}, 1,034 pg ml^{-1}, $P = 0.0244$) compared to controls (2,675 pg ml^{-1}), which suggests improved insulin sensitivity (**Fig. 3f**). Plasma C-peptide levels tended to be decreased after one month of treatment with Aib2 C24 lactam 40k or Aib2 C24 40k (738.8 pg ml^{-1}, 624.7 pg ml^{-1}) versus vehicle (1,077 pg ml^{-1}) ($P = 0.108$) (**Supplementary Fig. 9g**).

To determine whether the principal phenomenon generalizes across species, we administered both compounds to diet-induced obese rats (mean weight 777.4 ± 2.1 g, dose 70 nmol kg^{-1} week^{-1}, once-a-week injection, 3-week treatment). Aib2 C24 lactam 40k and Aib2 C24 40k each decreased body weight (for Aib2 C24 40k, –11.15 ± 0.88%; for Aib2 C24 lactam 40k, –20.58 ± 2.26%; for vehicle, 1.09 ± 0.56%) ($P < 0.0001$)
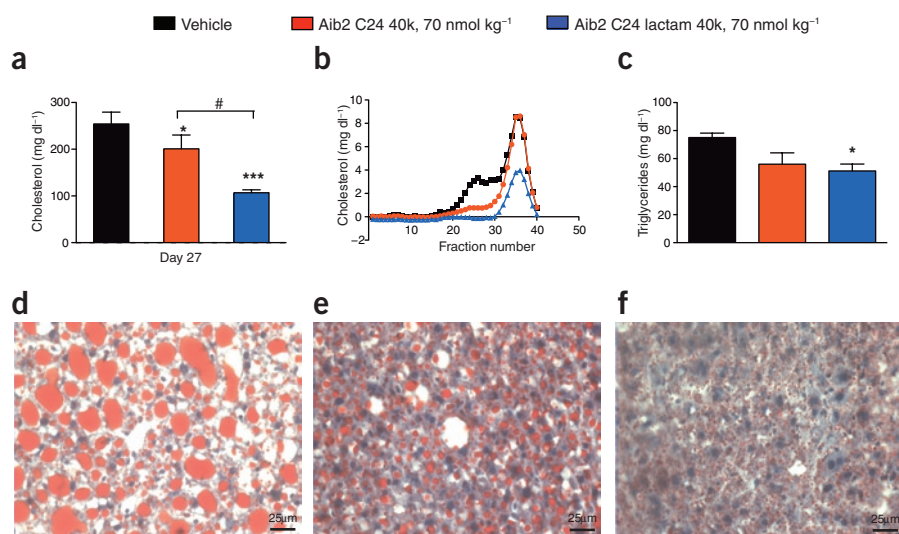
Figure 5 One-month treatment of diet-induced obese mice with glucagon and GLP-1 chimerae Aib2 C24 40k and Aib2 C24 lactam 40k. (**a–c**) Effects on plasma cholesterol (**a**), cholesterol FPLC (**b**) and triglycerides (**c**). Chronic effect on liver steatosis of diet-induced obese mice. (**d–f**) Vehicle (**d**), Aib2 C24 40k (**e**) and Aib2 C24 lactam 40k (**f**). *$P < 0.05$, ***$P < 0.001$; #$P < 0.05$ between treatment groups.

and fat mass of the DIO rats (for Aib2 C24 40k, $-19.17 \pm 2.03\%$; for Aib2 C24 lactam 40k, $-33.76 \pm 4.76\%$; for vehicle, $0.65 \pm 1.20\%$) ($P < 0.0001$), which confirms a species-independent applicability of this anti-obesity treatment approach (**Supplementary Fig. 10a,b**).

Chronic treatment improves lipid metabolism

Chronic subcutaneous treatment over 27 d with Aib2 C24 40k and Aib2 C24 lactam 40k decreased total cholesterol in DIO mice (200.8 ± 29.58 mg dl^{-1} and 106.9 ± 6.3 mg dl^{-1}, respectively) relative to vehicle (254.0 ± 25.33 mg dl^{-1}, $P = 0.0441$) (**Fig. 5a**). In a separate experiment, DIO mice subcutaneously received 70 nmol kg^{-1} of Aib2 C24 40k, Aib2 C24 lactam 40k or vehicle on days 0 and 7 and were evaluated on day 9. Aib2 C24 lactam 40k decreased plasma triglycerides, LDL cholesterol and total cholesterol (total cholesterol 63.0 $\pm$ 2.49 mg dl^{-1}, compared to vehicle 177.7 ± 11.8 mg dl^{-1}) ($P < 0.0001$), while potentially causing a shift from LDL to HDL cholesterol (**Fig. 5b**). Aib2 C24 40k decreased both LDL and HDL cholesterol but had no significant effect on triglycerides (**Fig. 5c**). There was a significant decrease in leptin ($3,343 \pm 723$ pg ml^{-1} for Aib2 C24 lactam 40k; $7,308 \pm 2,927$ pg ml^{-1} for Aib2 C24 40k; $18,642 \pm 6124$ pg ml^{-1} for vehicle; $P = 0.0426$), whereas no differences were observed

regarding plasma adiponectin and resistin levels (**Supplementary Fig. 11**). Chronic treatment for 27 d also normalized liver lipid content, while control DIO mice maintained substantial fatty liver disease (**Fig. 5d–f**).

Co-agonist activates hormone-sensitive lipase

We then tested the effects of a one-month treatment with Aib2 C24 40k or Aib2 C24 lactam 40k (**Fig. 6**). This treatment resulted in increased phosphorylation of hormone-sensitive lipase (HSL) in white adipose tissue (WAT) of DIO mice (Aib2 C24 40k, 1.135 ± 0.315; Aib2 C24 lactam 40k, 1.625 ± 0.149; vehicle, 0.597 ± 0.204; $P = 0.0369$) (**Fig. 6b,c**), which implies a glucagon-specific direct effect on WAT lipolysis since HSL activation is a known downstream signal of glucagon action. Concomitant with the decrease in fat mass of mice treated for two weeks at a dose of 35 nmol kg^{-1} week^{-1} with the Aib2 C24 lactam 40k and Aib2 C24 40k peptides, there was a substantial reduction of adipocyte size in epididymal adipose tissues when compared to control mice (**Supplementary Fig. 12**). However, despite having decreased fat mass and smaller adipocytes, this relatively short-term treatment of two weeks with the Aib2 C24 lactam 40k and Aib2 C24 40k peptides was not associated with a notable reduction of adipose tissue macrophage content, as quantified by real-time RT-PCR for CD68 (**Supplementary Fig. 10d**). Uncoupling protein 1 (UCP1) levels in brown adipose tissue (BAT) were increased by Aib2 C24 40k, but not by Aib2 C24 lactam 40k treatment (Aib2 C24 40k, 2.167 ± 0.429; Aib2 C24 lactam 40k, 1.287 ± 0.1558; vehicle, 1.0 ± 0.118; $P = 0.0264$) (**Fig. 6a**), which is consistent with a GLP-1–specific action on BAT resting thermogenesis. Hepatic gene expression reflective of hepatic gluconeogenesis was not affected by either Aib2 C24 40k or Aib2 C24 lactam 40k (**Supplementary Fig. 9h,i**). Histology indicated that pancreatic islets tended to be smaller following Aib2 C24 40k treatment (data not shown).

Co-agonist decreases adiposity in *Glp1r*$^{-/-}$ mice

In order to dissect the contributions of the GLP-1R and the GCGR agonist components of the Aib2 C24 40k and Aib2 C24 lactam 40k peptides, we administered them for one month to GLP-1 receptor knockout (*Glp1r*$^{-/-}$) mice[26] maintained on a high-fat diet. Aib2 C24 40k caused a nonsignificant reduction of body weight ($P > 0.05$) (**Fig. 7a,b**) and fat mass ($P > 0.05$) (**Fig. 7c**) compared to saline. In contrast, Aib2 C24 lactam 40k caused a significant decrease in body weight ($P = 0.0025$) and fat mass ($P = 0.0025$) in the *Glp1r*$^{-/-}$ mice (**Fig. 7b,c**). Aib2 C24 40k had no effect on food intake in *Glp1r*$^{-/-}$ mice, while Aib2 C24 lactam 40k suppressed food intake significantly ($P = 0.017$) (**Fig. 7d**). Aib2 C24 lactam 40k (but not Aib2 C24 40k) had a tendency to increase blood glucose in a glucose tolerance test in the absence of a functional GLP-1R ($P = 0.03$) (**Fig. 7e,f**), which implies that the GLP-1 component of the co-agonist is needed to protect against glucagon-induced hyperglycemia.
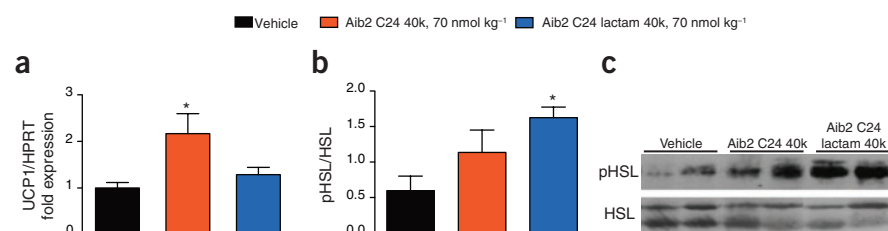

Figure 6 Lipolytic impact of glucagon and GLP-1 chimerae Aib2 C24 40k and Aib2 C24 lactam 40k. (**a**) Effects on BAT UCP1 expression levels. (**b,c**) Quantitative effect on phosphorylation of HSL in WAT. Shown are quantitative analysis relative to total HSL (**b**) and western blots (**c**). HPRT, hypoxanthine-guanine phosphoribosyltransferase (used as control). *$P < 0.05$.

DISCUSSION

Pharmacological treatment of obesity using single agents has limited efficacy[27] or presents risk for serious adverse effects[28,29]. No single agent has proven to be capable of reducing body weight more than 5–10% in the obese population[30]. Combination therapies using multiple drugs simultaneously may represent the preferred pharmaceutical approach to treat obesity, and there is ample precedent for combination therapy in treatment of chronic diseases. Here we present results that prove the principle that single molecules can be designed that are capable of simultaneously activating more than one mechanism to safely normalize body weight.

Glucagon is a peptide hormone best known for its insulin counter-regulatory actions. However, few reports have addressed chronic effects of increased glucagon agonism. Reasons for this limited pharmacological investigation include the limited solubility of the native peptide, its poor physical stability and its short duration of action. We have circumvented these constraints by creating glucagon agonists that are DPP-4 resistant and site-specifically PEGylated, allowing sustained pharmacology with infrequent weekly injections. The optimal level of glucagon agonism that achieves weight loss and lipolysis while minimizing hyperglycemia requires careful selection of dose and frequency of administration.

A set of high-potency glucagon-based co-agonists were generated that vary in selectivity with nearly a tenfold range of preference for one receptor or the other (**Table 1**). A single change in the C terminus of native glucagon or the Glu16 analog from acid to amide was observed to reduce selectivity for GCGR by approximately tenfold, with only a subtle decrease in potency at GCGR (**Table 1**). The molecular basis of this biochemical difference appears to be in part a function of increased conformational change associated with absence of the C-terminal negative charge (**Supplementary Fig. 1** and **Supplementary Table 1**). Chimera 1 (**14**) demonstrates an inverse preference in receptor activity relative to glucagon, where there is tenfold greater activity at GLP-1R compared to GCGR. Analysis of chimera 2 (**15**) restored potency at GCGR through the return of native glucagon residues Met27, Asn28 and Thr29.

We explored side chain–based lactams on the glucagon amide (**3**) backbone as a means to access backbone conformational preference. Each of the four peptide lactams studied (**26**, **27**, **28** and **29**) was well tolerated at both receptors and was more potent than glucagon amide. Lactam-based peptides **26** (Lys12-Glu16) and **27** (Glu16-Lys20) proved the most potent, and the former demonstrated that the positive charge at position 12 is not required for maximum potency in the presence of the 12–16 lactam.

A single Aib residue was substituted for the native serine of glucagon at position 2 as a means to suppress DPP-4–mediated N-terminal proteolysis. Further, site-specific PEGylation with a 40-kDa linear polymer was introduced at residue 24. The use of Aib2 in the glucagon-based peptide amide termed chimera 2 (**30**) selectively reduced the glucagon agonism relative to the native Ser2 (**15**) (**Table 1** and **Supplementary Fig. 6**). The peptide Aib2 C24 chimera 2 has full GLP-1 potency at GLP-1R, but only 10% of the potency of native glucagon at GCGR. The insertion of a backbone lactam between Glu16 and Lys20 in Aib2 C24 chimera 2 lactam (**32**) restored the glucagon agonism to a level comparable to that previously observed with Ser2 (**15**). Relative to native hormone, this peptide profile is one of a nearly balanced co-agonist, with full potency.
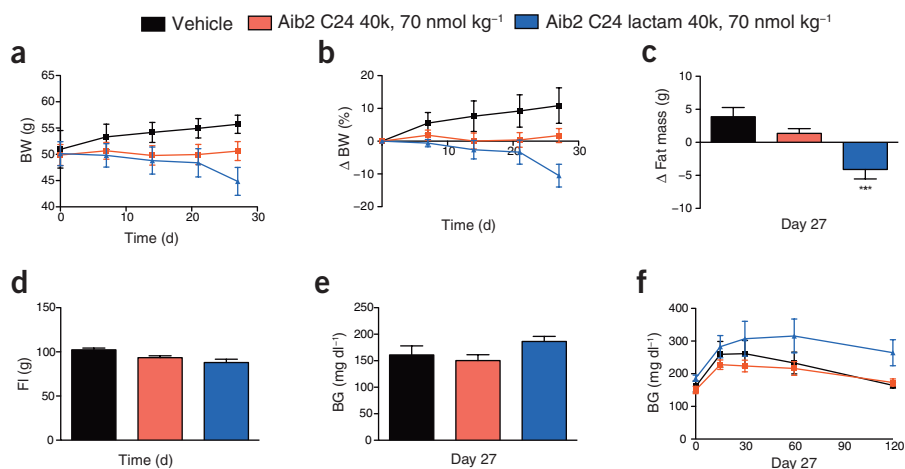

Figure 7 Effect of glucagon and GLP-1 chimerae Aib2 C24 40k and Aib2 C24 lactam in GLP-1R knockout mice. (**a**) Body weight. (**b**) Percent change in body weight. (**c**) Fat mass. (**d**) Food intake. (**e**) Fasting blood glucose. (**f**) Glucose tolerance. ***$P < 0.001$.

Weekly administration of the PEGylated peptides having different levels of relative agonism at the glucagon and GLP-1 receptors was highly effective in lowering adiposity and improving glucose tolerance of diet-induced obese mice. The peptide with balanced co-agonism proved especially efficacious, and within only a few weeks of therapy there was an apparent normalization of body weight and blood glucose. These preclinical studies indicate that a combination of the appetite-suppressing and insulin-release-promoting effects of GLP-1, when combined with the lipolytic effects of sustained glucagon receptor activation, successfully lowered body weight beyond the maximum that was achieved with the more selective GLP-1 agonist. The one-week dose titration study indicated an increased potency of approximately tenfold for the co-agonist peptide, where a 35 nmol kg^{-1} dose exceeded the body weight lowering achieved with 350 nmol kg^{-1} of the purer GLP-1 agonist (**Supplementary Fig. 8**). Additionally, the efficacy appeared to be maintained over the duration of the one-week study for the co-agonist, whereas the effect of the purer agonist appeared to reach a plateau at mid-week and a subsequent return toward vehicle control by day 7. Repeated dosing revealed a consistent dose response over the course of a month and a clear efficacy advantage in favor of the co-agonist (**Fig. 3**).

Notably, the hyperglycemia-promoting effects of glucagon that occur with acute administration were not observed with the co-agonist at any dose in either the one-week or the chronic study. There are several possible reasons for this: (i) the intrinsic GLP-1R agonism of these molecules opposes and potentially neutralizes any glucagon receptor-mediated diabetogenic effects; (ii) the considerable decrease in fat mass provides strong metabolic benefits that synergize to dominate any hyperglycemic drive; and (iii) sustained pharmacological glucagon receptor activation is an understudied phenomenon and is worthy of additional research in the absence of body weight lowering with GLP-1 co-agonism. In any event, our observations demonstrate that a well-equilibrated addition of glucagon receptor agonism to a GLP-1R agonist lowers body adiposity and improves glucose tolerance. Further studies are needed to determine the preferred ratio of GCGR:GLP-1R co-agonism for optimizing effects on blood glucose and body weight. **Supplementary Figure 10c** schematically indicates the principal importance of a balanced co-agonist ratio in order to achieve additive or even synergistic effects on adiposity, without sacrificing beneficial impact on glucose homeostasis.

The elimination of GLP-1 agonism through administration of the peptides to GLP-1 receptor knockout mice illustrated the absolute importance of GLP-1 receptor agonism and the relative contribution of glucagon receptor agonism. These experimental results point to the molecular basis for the enhanced efficacy observed with the co-agonist. What is more difficult to assess is whether the enhanced action is a direct function of two additive activities at separate tissues, or whether there exists a synergistic character to the chimeric co-agonist by virtue of activating two complementary receptors at the same tissue. An additional advantage of the combined single-molecule approach we present is the opportunity to work with lower total doses than with individual agonists. It seems reasonable to expect that lower drug exposure will minimize the risk for off-target adverse effects. This topic remains a target for future investigation.

The sustained activity profile of these compounds allowed for new insight into the physiology of energy balance regulation by gut hormones. Body-weight-lowering effects mediated by GLP-1R and GCGR appear to be mediated via distinct pathways, rather than through common signaling endpoints, thereby allowing for additive action. The impressive decrease in body adiposity achieved with the co-agonist chimera also suggests that the maximally achievable and sustainable body weight loss of 10%, as with currently available pharmaceutics, may not reflect an insurmountable physiological barrier. In fact, the present results indicate that complete normalization of body weight and insulin sensitivity in morbidly diet-induced obese mice is possible by co-agonism in a single peptide.

The present results trigger an array of new questions and the opportunity for further enhancement of the pharmacology. First, there is no reason to assume that the fine-tuned combination of these two particular gut hormones in a single molecule represents the only or optimal pharmacological approach to prevent or treat obesity. Second, it seems at least theoretically possible to include circulating factors other than gut hormones in an analogous single-molecule co-agonist. Finally, a combination of more than two endogenous metabolic control peptides into a single molecule may provide an even more potent action profile and could lead to receptor occupancy patterns more closely resembling physiological regulation.

METHODS

Lactam synthesis. Cyclized peptides with i to $i + 4$ lactam formation were synthesized on resin. Glu(OFm)-OH gamma ester (Peptides International) and Lys(Fmoc)-OH (Peptides International) were substituted for Glu(OcHex) and Lys(2-Cl–Z) at positions involved in lactam formation. The fully protected peptidyl-resin was treated with 20% piperidine (v/v) in dimethylformamide for 45 min to remove Fmoc and OFm protecting groups. On-resin lactam formation was achieved after treatment with 5 equivalents of benzotriazole-1-yl-oxy-tris-pyrrolidinophosphonium hexafluorophosphate (PyBOP) (Fluka) in dimethylformamide with diisopropylethylamine for 5 h. Lactam formation was confirmed by ninhydrin analysis and mass reduction of 18 relative to the open form of the peptide.

PEGylation of peptides. Purified peptides were mixed at a 1:1 molar ratio with methoxy poly(ethylene glycol) maleimido-propionamide-40K (Chirotech Technology Ltd) in 7 M urea and 50 mM Tris, pH 8.0. Reaction progress was monitored by analytical reverse-phase HPLC, and free peptide was consumed within 30 min. The reaction was quenched in 0.1% (v/v) trifluoroacetic acid, purified and characterized.

Glucagon and GLP-1 receptor-mediated cAMP synthesis. Each peptide analog was tested for its ability to stimulate cAMP production through the glucagon and GLP-1 receptors. Human embryonic kidney (HEK293) cells were co-transfected with the GCGR or GLP-1R cDNAs and a luciferase reporter gene linked to a cAMP response element (CRE). Cells were serum deprived for 16 h

by culturing in DMEM (Invitrogen) supplemented with 0.25% (v/v) bovine growth serum (HyClone). Serial dilutions of glucagon and GLP-1 analogs were added to 96-well poly-D-lysine–coated plates (BD Biosciences) containing co-transfected HEK293 cells, and plates were incubated for 5 h at 37 °C, 5% CO_2. Following incubation, an equivalent volume (100 µl) of LucLite luminescence substrate reagent (Perkin-Elmer) was added to each well and the plate was shaken for 3 min at 800 r.p.m. The plate was incubated for 10 min in the dark, and light output was quantified on a MicroBeta-1450 liquid scintillation counter (Perkin-Elmer). EC_{50} values were calculated by Origin software (OriginLab).

Circular dichroism measurements. Peptides were dissolved in 10 mM phosphate buffer pH 5.9 with increasing concentrations of TFE, and peptide concentrations were quantified by measuring absorbance at 276 nm. Each sample was diluted to 10 µM for CD measurements. CD data were collected on a JASCO J-715 circular dichroism spectropolarimeter with constant nitrogen stream and temperature control of the 1 mm path length cell set at 25 °C. Spectral data were accumulated for 5 scans from 270 to 190 nm with a scan speed of 100 nm min^{-1} and 1 nm wavelength step. Solvent signal was subtracted and data were smoothed[31] in the JASCO Spectra Manager software. Millidegree values obtained were converted to mean residue ellipticity with units of deg cm^2 dmol^{-1}. Calculated mean residue ellipticity values were input into DICHROWEB[32,33] CDSSTR algorithm to obtain percent helicity values.

Animals. C57Bl/6 mice were obtained from Jackson Laboratories and fed a diabetogenic diet from Research Diets: a high-sucrose diet with 58% kcal from fat. Mice were single or group-housed on a 12:12-h light-dark cycle at 22 °C with free access to food and water. All studies were approved by and performed according to the guidelines of the Institutional Animal Care and Use Committee of the University of Cincinnati.

Body composition measurements. Whole-body composition (fat and lean mass) was measured using NMR technology[34] (EchoMRI).

Energy balance physiology measurements. Energy intake and expenditure, as well as home-cage activity, were assessed by using a combined indirect calorimetry system (TSE Systems). O_2 consumption and CO_2 production were measured every 45 min for a total of 120 h (including 12 h of adaptation) to determine the respiratory quotient and energy expenditure. Food intake was determined continuously for 120 h at the same time as the indirect calorimetry assessments by integration of scales into the sealed cage environment. Home-cage locomotor activity was determined using a multidimensional infrared light beam system with beams scanning the bottom and top levels of the cage, and activity being expressed as beam breaks.

Blood parameters. Blood was collected after a 6-h fast from tail veins using EDTA-coated Microvette tubes (Sarstedt) and immediately chilled on ice. After 15 min of centrifugation at 3,000g and 4 °C, plasma was stored at –80 °C. Plasma insulin was quantified by a radioimmunoassay from Linco (Sensitive Rat Insulin RIA; Linco Research). Plasma triglycerides and cholesterol levels were measured by enzymatic assay kits (Thermo Electron). Samples were analyzed individually with the exception that pooled samples (0.25 ml) from 5 animals per group were subjected to fast-performance liquid chromatography (FPLC) gel filtration on two Superose 6 columns connected in series for lipoprotein separation. All assays were performed according to the manufacturers' instructions.

Glucose tolerance test. For the determination of glucose tolerance, mice were subjected to 6 h of fasting and injected intraperitoneally with 2 g glucose per kg body weight (20% w/v D-glucose (Sigma) in 0.9% w/v saline). Tail blood glucose levels (mg dl^{-1}) were measured by using a handheld glucometer (TheraSense Freestyle) before (0 min) and at 15, 30, 60, 90 and 120 min after injection.

Statistical analyses. Unless indicated otherwise, all statistical analyses were performed using GraphPad Prism. The analysis of the results obtained in the *in vivo* experiments was performed using one-way ANOVAs followed by Tukey *post hoc* tests. P values lower than 0.05 were considered significant. The results are presented as means ± s.e.m. of 7–8 replicates per group. Receptor activation data is ± s.d.

Other methods. See **Supplementary Methods** for descriptions of peptide synthesis and characterization, staining and labeling procedures, and RT-PCR protocol and primer sequences.

Accession codes. Protein Data Bank: The crystal structure of Ex-4 (9–39) with the N-terminal extracellular domain of the GLP-1 receptor was deposited with accession code 3C5T as part of a previous study. The crystal structure of glucagon was deposited with accession code 1GCN as part of a previous study.

Note: Supplementary information is available on the Nature Chemical Biology website.

1. Ogden, C.L. *et al.* Prevalence of overweight and obesity in the United States, 1999–2004. *JAMA* **295**, 1549–1555 (2006).
2. Neovius, M. & Narbro, K. Cost-effectiveness of pharmacological anti-obesity treatments: a systematic review. *Int. J. Obes.* **32**, 1752–1763 (2008).
3. Cvetkovic, R.S. & Plosker, G.L. Exenatide - a review of its use in patients with type 2 diabetes mellitus (as an adjunct to metformin and/or a sulfonylurea). *Drugs* **67**, 935–954 (2007).
4. Gutniak, M., Orskov, C., Holst, J.J., Ahren, B. & Efendic, S. Antidiabetogenic effect of glucagon-like peptide-1 (7–36)amide in normal subjects and patients with diabetes-mellitus. *N. Engl. J. Med.* **326**, 1316–1322 (1992).
5. Roth, J.D. *et al.* Leptin responsiveness restored by amylin agonism in diet-induced obesity: evidence from nonclinical and clinical studies. *Proc. Natl. Acad. Sci. USA* **105**, 7257–7262 (2008).
6. Woods, S.C., Lutz, T.A., Geary, N. & Langhans, W. Pancreatic signals controlling food intake; insulin, glucagon and amylin. *Philos. Trans. R. Soc. Lond. B Biol. Sci.* **361**, 1219–1235 (2006).
7. Geary, N., Kissileff, H.R., Pisunyer, F.X. & Hinton, V. Individual, but not simultaneous, glucagon and cholecystokinin infusions inhibit feeding in men. *Am. J. Physiol.* **262**, R975–R980 (1992).
8. Geary, N. Pancreatic glucagon signals postprandial satiety. *Neurosci. Biobehav. Rev.* **14**, 323–338 (1990).
9. Geary, N. Glucagon and the control of meal size. in *Satiation: From Gut To Brain* (ed. Smith, G.P.) 164–197 (Oxford University Press, USA, 1998).
10. Goodridge, A.G. & Ball, E.G. Studies on metabolism of adipose tissue .18. In vitro effects of insulin epinephrine and glucagon on lipolysis and glycolysis in pigeon adipose tissue. *Comp. Biochem. Physiol.* **16**, 367–381 (1965).
11. Heckemeyer, C.M., Barker, J., Duckworth, W.C. & Solomon, S.S. Studies of the biological effect and degradation of glucagon in the rat perifused isolated adipose cell. *Endocrinology* **113**, 270–276 (1983).
12. Davidson, I.W.F., Salter, J.M. & Best, C.H. The effect of glucagon on the metabolic rate of rats. *Am. J. Clin. Nutr.* **8**, 540–546 (1960).
13. Salter, J.M. Metabolic effects of glucagon in the Wistar rat. *Am. J. Clin. Nutr.* **8**, 535–539 (1960).
14. Chan, E.K. *et al.* Suppression of weight-gain by glucagon in obese Zucker rats. *Exp. Mol. Pathol.* **40**, 320–327 (1984).
15. Hjorth, S.A., Adelhorst, K., Pedersen, B.B., Kirk, O. & Schwartz, T.W. Glucagon and glucagon-like peptide 1: selective receptor recognition via distinct peptide epitopes. *J. Biol. Chem.* **269**, 30121–30124 (1994).
16. Orskov, C. Glucagon-like peptide-1, a new hormone of the enteroinsular axis. *Diabetologia* **35**, 701–711 (1992).
17. Wynne, K. *et al.* Subcutaneous oxyntomodulin reduces body weight in overweight and obese subjects - a double-blind, randomized, controlled trial. *Diabetes* **54**, 2390–2395 (2005).
18. Baggio, L.L., Huang, Q.L., Brown, T.J. & Drucker, D.J. Oxyntomodulin and glucagon-like peptide-1 differentially regulate murine food intake and energy expenditure. *Gastroenterology* **127**, 546–558 (2004).
19. Small, C.J. & Bloom, S.R. Gut hormones and the control of appetite. *Trends Endocrinol. Metab.* **15**, 259–263 (2004).
20. Cohen, M.A. *et al.* Oxyntomodulin suppresses appetite and reduces food intake in humans. *J. Clin. Endocrinol. Metab.* **88**, 4696–4701 (2003).
21. Billington, C.J., Bartness, T.J., Briggs, J., Levine, A.S. & Morley, J.E. Glucagon stimulation of brown adipose-tissue growth and thermogenesis. *Am. J. Physiol.* **252**, R160–R165 (1987).
22. Runge, S. *et al.* Three distinct epitopes on the extracellular face of the glucagon receptor determine specificity for the glucagon amino terminus. *J. Biol. Chem.* **278**, 28005–28010 (2003).
23. Runge, S., Wulff, B.S., Madsen, K., Brauner-Osborne, H. & Knudsen, L.B. Different domains of the glucagon and glucagon-like peptide-1 receptors provide the critical determinants of ligand selectivity. *Br. J. Pharmacol.* **138**, 787–794 (2003).
24. Neidigh, J.W., Fesinmeyer, R.M., Prickett, K.S. & Andersen, N.H. Exendin-4 and glucagon-like-peptide-1: NMR structural comparisons in the solution and micelle-associated states. *Biochemistry* **40**, 13188–13200 (2001).
25. Runge, S., Thogersen, H., Madsen, K., Lau, J. & Rudolph, R. Crystal structure of the ligand-bound glucagon-like peptide-1 receptor extracellular domain. *J. Biol. Chem.* **283**, 11340–11347 (2008).
26. Scrocchi, L.A. *et al.* Glucose intolerance but normal satiety in mice with a null mutation in the glucagon-like peptide 1 receptor gene. *Nat. Med.* **2**, 1254–1258 (1996).
27. Rucker, D., Padwal, R., Li, S.K., Curioni, C. & Lau, D.C.W. Long term pharmacotherapy for obesity and overweight: updated meta-analysis. *BMJ* **335**, 1194–1199 (2007).
28. Christensen, R., Kristensen, P.K., Bartels, E.M., Blidda, H. & Astrup, A. Efficacy and safety of the weight-loss drug rimonabant: a meta-analysis of randomised trials. *Lancet* **370**, 1706–1713 (2007).
29. Griffen, L. & Anchors, M. Asymptomatic mitral and aortic valve disease is seen in half of the patients taking 'Phen-Fen'. *Arch. Intern. Med.* **158**, 102 (1998).
30. Amori, R.E., Lau, J. & Pittas, A.G. Efficacy and safety of incretin therapy in type 2 diabetes - systematic review and meta-analysis. *JAMA* **298**, 194–206 (2007).
31. Savitzky, A. & Golay, M.J.E. Smoothing and differentiation of data by simplified least squares procedures. *Anal. Chem.* **36**, 1627–1639 (1964).
32. Whitmore, L. & Wallace, B.A. Protein secondary structure analyses from circular dichroism spectroscopy: methods and reference databases. *Biopolymers* **89**, 392–400 (2008).
33. Whitmore, L. & Wallace, B.A. DICHROWEB, an online server for protein secondary structure analyses from circular dichroism spectroscopic data. *Nucleic Acids Res.* **32**, W668–W673 (2004).
34. Tinsley, F.C., Taicher, G.Z. & Heiman, M.L. Evaluation of a quantitative magnetic resonance method for mouse whole body composition analysis. *Obes. Res.* **12**, 150–160 (2004).